Preparation and characterization of zirconia nanoparticles infused carboxymethyl cellulose hydrogel and their antimicrobial evaluation

Chaitanya Raj Naharki[*,], Nelson Rai[**,***,****], Manish Man Shrestha[**,***,****], Shankar P. Khatiwada[*,**,****], Kshama Parajuli[***], Rameshwar Adhikari[**,***,****] and Rajesh Pandit[*,**,****]**

[*] Department of Chemistry, Tri-Chandra Multiple Campus, Tribhuvan University, Ghantaghar, Kathmandu, Nepal.

[**]Research Centre for Applied Science and Technology (RECAST), Tribhuvan University, Kirtipur, Kathmandu, Nepal.

[***] Central Department of Chemistry, Tribhuvan University, Kirtipur, Kathmandu, Nepal.

[****]Nepal Polymer Institute (NPI), P. O. Box 24411, Kathmandu, Nepal.

Abstract: In this study, the preparation of zirconia (ZrO_2) nanoparticles (NPs) infused carboxymethyl cellulose (CMC) hydrogel films. CMC hydrogel was prepared by adding citric acid (CA) to the CMC solution. The ZrO_2 NPs were synthesized by the sol-gel method and modified using ascorbic acid (AA) and CA. The modified ZrO_2 NPs suspension was incorporated into the CMC hydrogel paste to prepare zirconia-infused CMC hydrogel films (ZCMCH). The prepared ZCMCH was characterized using FTIR, UV-Visible, XRD, and SEM. The stretching vibrations in the wavenumber range of 450-750 cm^{-1} in FTIR analysis confirmed the successful formation of ZrO_2 NPs. XRD analysis revealed an average crystallite size of 10.80 nm for ZrO_2 NPs, and the diffractogram of ZCMCH exhibited characteristic peaks at 2θ values of approximately 16°, 29°, and 40°, confirming the incorporation of ZrO_2 NPs within the CMC hydrogel matrix. SEM analysis confirmed the proper distribution of ZrO_2 NPs throughout the CMC hydrogel matrix with an average particle diameter of 4.81 μm. Furthermore, the ZCMCH was evaluated for antimicrobial analysis against selected microbial strains, bacteria (*Escherichia coli* and *Bacillus subtilis*), and fungus (*Candida albicans*). The antimicrobial efficacy of the samples was assessed by the agar well diffusion method, showing an inhibition zone of 1.6 cm against bacteria and 1.4 cm against fungus. These findings suggest that the developed ZrO_2 NPs infused CMC hydrogel holds considerable potential for biomedical applications.

Keywords: Antimicrobial; FTIR; Hydrogel; SEM; XRD; ZrO_2 NPs.

Introduction

Hydrogels are three-dimensional, cross-linked, hydrophilic, branched, or linear polymers that are super-absorbent. They can imbibe water, physiological, or saline solutions[1]. Hydrogels can be classified into two types: natural polymer-based hydrogels and synthetic polymer-based hydrogels. Natural polymer-based hydrogels have recently supplanted synthetic polymer-based materials due to several benefits, like biocompatibility, biodegradability, and no hazardous chemicals are formed during the process of decomposition[2].

Cellulose is one of the most abundant existing natural polymers that can be used for the preparation of cellulose-based hydrogels[3]. The hydroxyl groups in cellulose-based hydrogels have a strong capacity to establish hydrogen bonds and play an important role in their ability to retain large amounts of water or nutrients for a longer time[4].

Author for correspondence: Rajesh Pandit, Department of Chemistry, Tri-Chandra Multiple Campus, Tribhuvan University, Kathmandu, Nepal.
Email: rajesh.pandit@trc.tu.edu.np; https://orchid.org/ 0000-0002-6663-8950
Received: 8 Jan, 2026; Received in revised form: 15 Apr, 2026; Accepted: 17 Apr, 2026.
Doi: https://doi.org/10.3126/sw.v19i19.95630

Since the cellulose does not itself dissolve in water, its derivative, namely, carboxymethyl cellulose (CMC), being water soluble, is used for the preparation of cellulose-based hydrogels[5].

CMC has a lot of carboxymethyl groups attached to the cellulose backbone[6]. The most important step in creating a hydrogel is cross-linking, which holds the 3D structure and improves the physical and mechanical characteristics of the hydrogel[7]. The hydrophilic nature of CMC makes it practicable to blend and crosslink with various materials such as natural polymers, synthetic polymers, and inorganic materials[8]. Different cross-linking procedures, like physical, chemical, and polymerization methods, are used to make hydrogel from cellulose and its derivatives[7]. Among these, chemical cross-linking is now the most common approach for making CMC hydrogel[9]. Recently, there have been many reports of enhanced performance of CMC hydrogel by the inclusion of metal oxide NPs. Because of unique optical, electrical, mechanical, and structural properties, ZrO_2 NPs have appeared as promising filler materials in the fabrication of nanocomposites (NCs)[10, 11].

NPs play a significant role in modifying the polymer matrix during the formation of NCs. To increase the dispersion of NPs, surface modification with different modifiers has received significant attention. The use of unmodified metal oxides like zirconia NPs for NCs preparation was restricted to low NPs concentrations because NPs aggregation (due to Van der Waals attraction) precludes proper dispersion into the polymer matrix[12].

Biosafe organic compounds, such as ascorbic acid (AA) and citric acid (CA), have been used for surface modification of metal oxides and to enhance the biocompatibility and biodegradability of the organic polymers, as well as for the dispersion of NPs[12, 13]. AA contains 4 hydroxyl (–OH) groups, whereas CA contains three –OH groups that can bind to metal oxides and function as a cross-linking agent[7, 12]. The hydrophilicity and porosity of hydrogels make them suitable for antibacterial applications. Also, ZrO_2 NPs themselves can exhibit antimicrobial properties[14]. Therefore, hydrogels containing inorganic antimicrobial materials can both improve their antimicrobial capabilities and sustain antimicrobial activity for a very long time[15]. Since too many drug-resistant bacteria have emerged because of the improper use of antibiotics and other antimicrobial medications, hydrogel as an antimicrobial biomaterial may be a more flexible and adaptable option than conventional antibiotics[16].

In this paper, ZCMCH was fabricated for its antibacterial and antifungal activity. These prepared samples were characterized and investigated for their antibacterial activities against the gram-positive bacteria *Bacillus subtilis (B. subtilis)* and the gram-negative bacteria *Escherichia coli (E. coli),* including antifungal activities against the fungi *Candida albicans (C. albicans).*

Materials and methods

Materials

Chemicals used in this experiment, such as zirconium oxychloride octahydrate ($ZrOCl_2.8H_2O$), sodium hydroxide (NaOH), citric acid ($C_6H_8O_7$), and ascorbic acid ($C_6H_8O_6$) were manufactured by Himedia Laboratories Pvt. Ltd., India, and CMC powder was taken from Cellulose Solutions Private Limited, India, purchased from local suppliers in Kathmandu, Nepal. All chemical materials were used without any further purification.

Methods

Synthesis of ZrO_2 NPs

$ZrOCl_2.8H_2O$ was used as a precursor material for the preparation of ZrO_2 NPs. The precipitation of Zirconium hydroxide, $Zr(OH)_4$, was obtained by slowly adding 0.2 M NaOH (5 drops per minute) to the aqueous solution of 0.05 M $ZrOCl_2.8H_2O$ at room temperature, while continuously stirring with a magnetic stirrer until the milky white solution formed. The pH was maintained at 10.58. After the procedure was completed, the solution was kept at room temperature for 24 hours for aging. Then, the solution was filtered using Whatman filter paper No. 42. A whitish gel was obtained as a residue, which was thoroughly washed using distilled water until a neutral pH was achieved and

dried in a hot air oven for 3 hours at 80 °C. The final product was crushed by mortar and pestle and kept for 6 hours in a muffle furnace at 600 °C for calcination. Finally, the white powder was obtained as zirconia NPs[17, 18]. Figure 1 illustrates the process of ZrO_2 NPs synthesis, beginning with the titration.

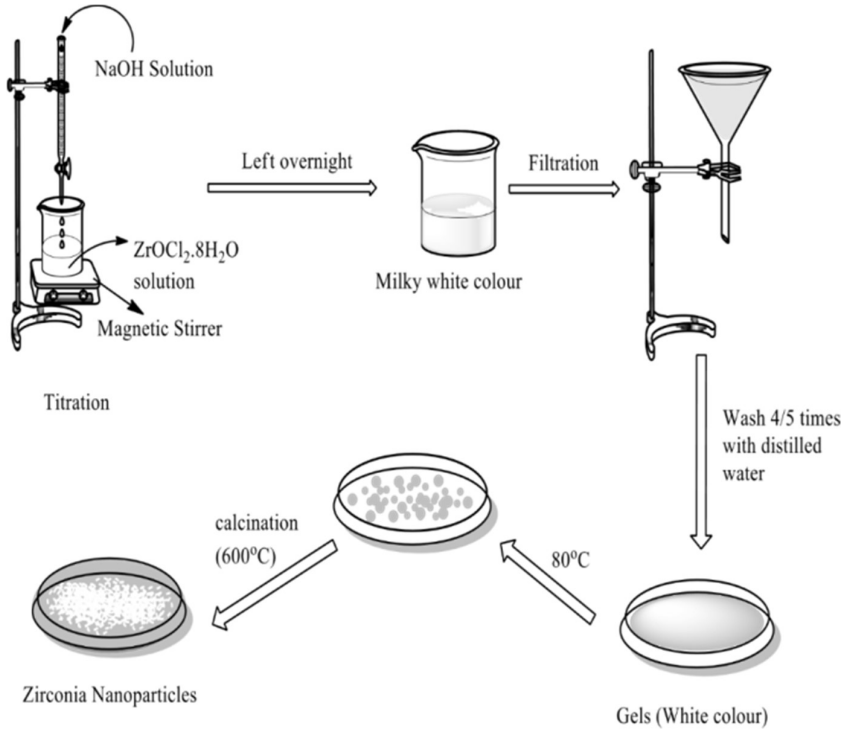

Figure 1: Schematic representation of the synthesis of ZrO_2 NPs.

Surface Modification of ZrO_2

For better homogeneous distribution of ZrO_2 NPs in the polymer matrix, the surface modification of the ZrO_2 NPs has been performed. In the first step, 0.10 g of ZrO_2 NPs was dispersed in 20 mL of distilled water and ultrasonicated for 30 minutes. Then, 0.02 g of citric acid and 0.02 g of AA were dissolved in 20 mL of distilled water separately, and each of them was ultrasonicated for 30 minutes to achieve homogeneous solutions. In the second step, the CA solution was added to the ZrO_2 suspension and ultrasonicated for 30 minutes. After that, the AA solution was added to the ZrO_2–CA suspension and ultrasonicated for 60 minutes to prepare the modified ZrO_2[19]. Figure 2 displays the process of surface modification of ZrO_2 NPs using CA and AA

Preparation of CMC hydrogel

1 g of CMC was dissolved in 30 mL of distilled water, and 0.075 g citric acid was dissolved in another 30 mL with continuous stirring using a magnetic stirrer. The citric acid solution was added dropwise to the CMC solution with continuous stirring at 60 °C for 60 minutes. The formed viscous solution was transferred to a petri plate, left at room temperature for 48 hours, and then dried in an oven at 35 °C for 420 minutes[20].

Preparation of ZrO_2 NPs infused CMC hydrogel

The modified ZrO_2 (5% relative to the CMC powder) was added to a CMC-CA paste-like solution and stirred for 60 minutes to form an optimal mixture of modified ZrO_2 NPs-CMC-CA. The solution was then poured into a petri dish and left at room temperature for 48 hours. It was then stored for 420 minutes at 35 °C in a hot air oven. A pale brownish-yellow thin film layer was produced[1]. Figure 3 demonstrates the overall preparation of ZrO_2 NPs infused CMC hydrogel.

Antimicrobial assay

Microbial strains of *Escherichia coli* (Gram-negative bacteria) ATCC8739, *Bacillus subtilis* (Gram-positive bacteria), ATCC 6051, and *Candida albicans* (Human

pathogenic fungi) ATCC 2091 were cultured in liquid broth (LB) media. The Mueller-Hinton Agar (MHA) plates were prepared, and the mixture was autoclaved at 15 psi pressure at 121 °C for 25 minutes. The sterilized media was cooled down to 40-50 °C, followed by transferring into petri dishes (25 mL each). Liquid bacterial seed was spread with the help of a sterile cotton swab on the surface of the media plates. The wells were made on the surface of agar, and ZCMCH (0.00284 g) and the standard kanamycin solution (5 mg/mL, 10 µL loaded) and standard itraconazole solution (20 mg/mL, 10 µL loaded) were used as a positive control for antibacterial and antifungal activities, respectively. The media plates were then incubated for 24 hrs at 37 °C. The zone of inhibition of antimicrobial test results was observed after 24 hours.

Characterization Techniques

UV–Visible Spectroscopy

UV–Visible spectroscopy was conducted to study the optical absorbance characteristics of ZrO_2 NPs and modified ZrO_2 NPs. The measurements were carried out using a UV–Visible spectrophotometer (Shimadzu UV-1900i, Japan) equipped with a 10 mm quartz cuvette. A deuterium lamp served as the UV light source, and a 20 W halogen lamp was used for the visible range. A silicon diode detector recorded the spectra within a wavelength range of 190–800 nm.

Fourier Transform Infrared (FTIR) Spectroscopy

FTIR analysis was performed using an IR Affinity-1

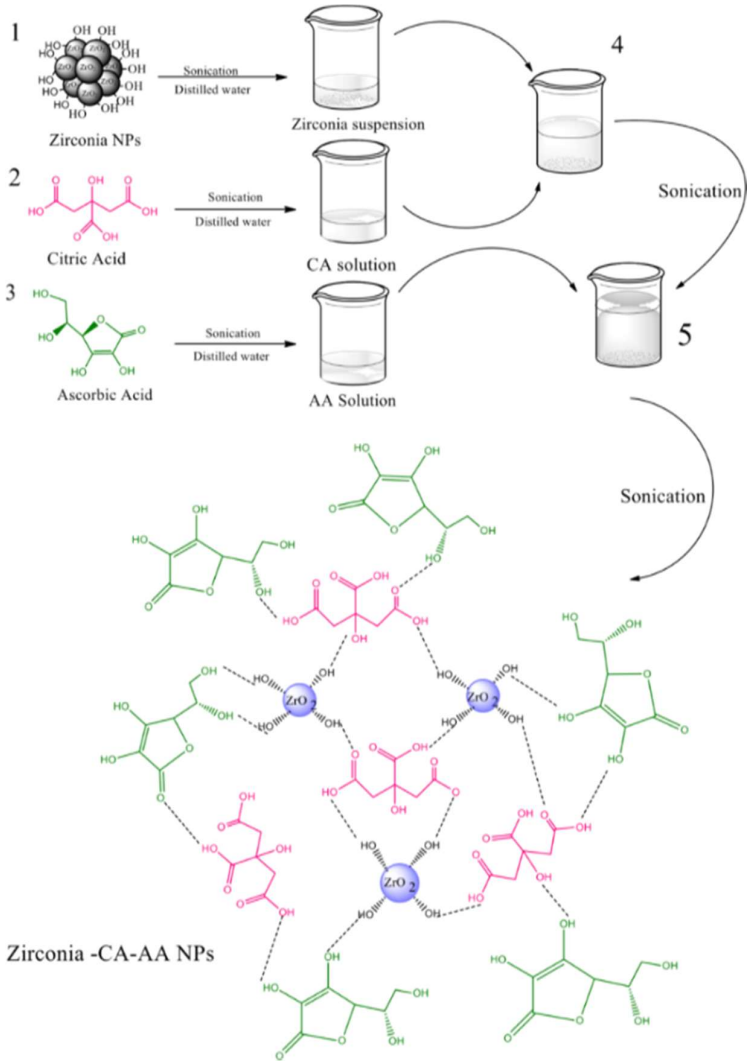

Figure 2: Schematic flowchart showing the functionalization of ZrO_2 NPs with CA and AA.

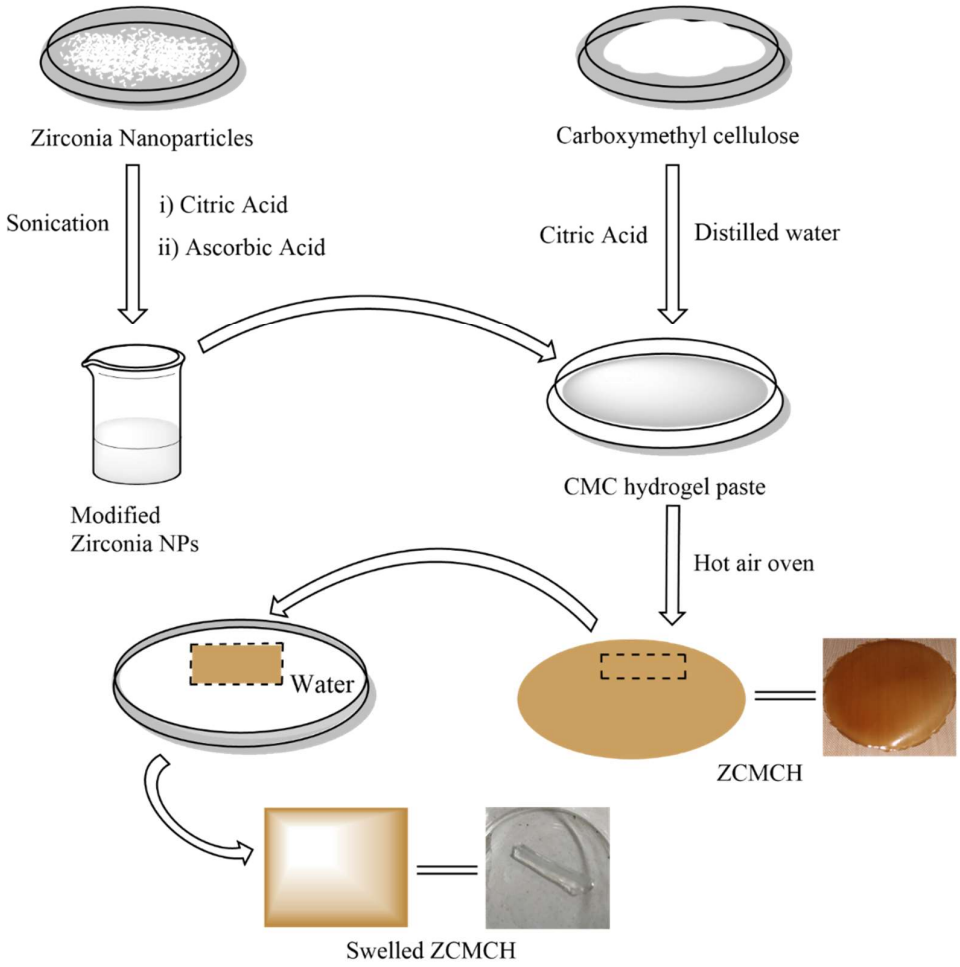

Figure 3: Schematic representation of the preparation of ZrO_2 NPs infused CMC hydrogel.

spectrophotometer (Shimadzu, Japan) to identify functional groups, species, and vibrational modes. The spectra were recorded in the range of 4000–400 cm^{-1} with a resolution of 4 cm^{-1}.

X-ray Diffraction (XRD) Analysis

The crystalline phase and structure of the samples were analysed using an X-ray diffractometer (Bruker D2 Phaser) with a monochromatic Cu Kα radiation source (λ = 0.15418 nm). Scans were recorded over a 2θ range of 20° to 80° at the Nepal Academy of Science and Technology (NAST), Nepal. The instrument was operated at 30 kV accelerating voltage and 10 mA emission current. Crystallite sizes were calculated using the Debye-Scherrer equation.

Scanning Electron Microscopy (SEM)

Surface morphology of ZrO_2-infused CMC hydrogel was examined by scanning electron microscopy (SEM). Samples were coated with a 20 nm gold layer to enhance conductivity and image resolution. SEM analysis was performed using a Camscan 44 microscope with an accelerating voltage of 20 kV, and images were captured at a working distance of 39 mm.

Results and Discussion

UV-Visible Spectroscopy

The UV-Visible spectra of pure ZrO_2 NPs and modified ZrO_2 NPs were acquired in the wavelength region of 200-400 nm. There is no peak observed in the range of (270-320) nm for pure ZrO_2 NPs, while modified ZrO_2 NPs exhibit a sharp and noticeable peak at about 292 nm in their UV-Visible absorption spectrum, as shown in Figure 4. A similar kind of result has been demonstrated in the given literature[21]. The spectrum of pure ZrO_2 has no peak due to

agglomeration of particles in pure ZrO_2; in contrast, modified ZrO_2 exhibits good nanoparticle dispersion. The obtained UV-visible spectra of modified ZrO_2 NPs and pure ZrO_2 NPs demonstrate that the dispersion of ZrO_2 NPs is enhanced via modification using CA and AA[19].

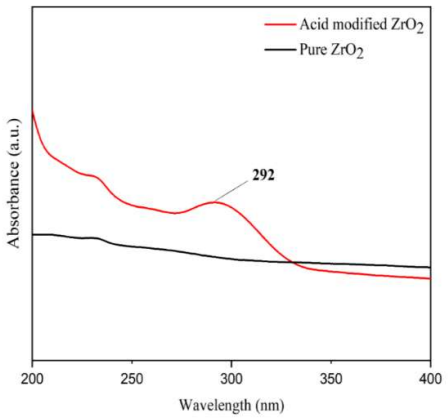

Figure 4: UV- Visible spectra of pure ZrO_2 and modified ZrO_2 NPs.

Fourier Transform Infrared (FTIR) Spectroscopy

The synthesized ZrO_2 NPs *via* the sol-gel technique were analysed by FTIR to identify the functional group present in the particles, as shown in Figure 5. The spectra in the region of 500-750 cm^{-1} show the characteristic of the tetragonal Zr-O-Zr vibration[22, 23]. The peak at 482 cm^{-1} was assigned to the Zr-O vibration, confirming the synthesis of the ZrO_2 structure. The peak observed at 1515 cm^{-1} may be related to adsorbed moisture. The band at 3525 cm^{-1} corresponds to the hydroxyl groups[11, 23]. Further, the ending vibrations of absorbed water molecules connected to the ZrO_2 NPs are present at 1628 cm^{-1}. Identical peak positions were reported in the literature[19]. Hence, the peak obtained by FTIR is in good agreement with the literature report, which confirmed the formation of ZrO_2 nanostructures[11, 22, 23].

The FTIR spectrum was compared for identifying pure materials, pure CMC, and ZrO_2 NPs infused CMC hydrogel. Figure 6 displays the properties of the absorption peaks for CMC and ZrO_2 NPs infused CMC hydrogel. The bands observed in the 1000–1200 cm^{-1} region were assigned to the –C–O– stretching on the polysaccharide skeleton[24]. The absorption bands in the range 450–750 cm^{-1} are due to Zr-O vibration modes, which confirmed the bending of ZrO_2 NPs in CMC hydrogel[23]. The peak at 1415 cm^{-1} is related to $-CH_2$ scissoring vibrations, and asymmetrical stretching vibrations of the carboxylate groups are associated with the peaks at 1587 cm^{-1}. The stretching vibration of –C–O–C– stretching vibration has a peak at 1323 cm^{-1}[25, 1]. The stretching vibration of the hydroxyl group –OH in ZrO_2 NPs infused CMC hydrogel was identified at around 3375 cm^{-1}, and the peak at 2920 cm^{-1} is the characteristic C-H stretching of $-CH_2$ (from both CMC and ZCMCH) that hints at the formation of ZrO_2 NPs infused CMC hydrogel.

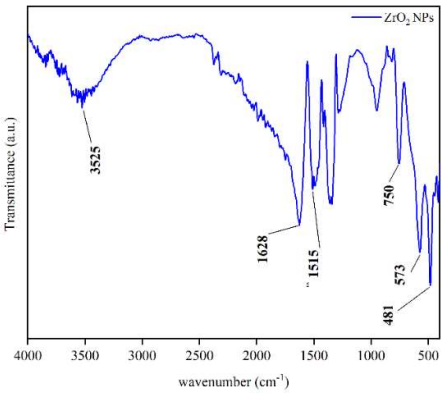

Figure 5: FITR spectrum of ZrO_2 NPs.

X-Ray Diffraction Analysis

X-ray diffraction (XRD) analysis was used to investigate the structure of pure zirconia nanoparticles (ZrO_2 NPs), pure carboxymethyl cellulose (CMC) hydrogel, and the ZCMCH are shown in Figure 7. The XRD pattern of pure ZrO_2 nanoparticles exhibits distinct peaks at different positions with varying intensities across all samples. In the case of zirconia NPs, diffraction peaks were seen at approximately $2\theta \approx 30.18°$,

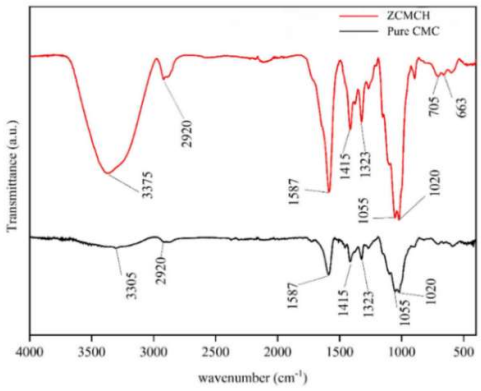

Figure 6: FTIR spectra of pure CMC and ZCMCH.

35.11˚, 50.28˚, and 59.94°, which can be indexed to the respective (hkl) values were found to be (101), (110), (112), and (211) planes, respectively, confirming the formation of crystalline tetragonal zirconia and were in good agreement with the literature report[11, 26]. The obtained XRD result was further used to obtain the crystallite size of the prepared zirconia NPs using Debye-Scherrer's equation. The average crystallite size of the synthesized ZrO_2 NPs was found to be 10.80 nm, and the relatively broadened nature of these peaks indicates the disordered fraction of the zirconia particles. Table 1 illustrates the peak position, full-width half maximum (FWHM), grain size, hkl values, and average crystalline size. In contrast, the XRD pattern of the pure CMC hydrogel displays a broad diffuse peak centred around 2θ ≈ 18–22°, characteristic of an amorphous polymeric structure with no long-range crystalline order. For the ZCMCH composite, the diffraction pattern was dominated by the amorphous background of CMC, while the characteristic zirconia peaks were significantly reduced in intensity and partially broadened. This reduction was attributed to the homogeneous dispersion of zirconia nanoparticles within the polymer matrix and the dilution effect of the amorphous hydrogel phase. Mostly, no additional diffraction peaks were observed in the composite, indicating that no new crystalline phases were formed during composite preparation. These results confirm the successful incorporation of nanocrystalline zirconia into the CMC hydrogel while preserving the structural characteristics of both components[25, 27].

Scanning Electron Microscopy (SEM)

SEM analysis was used to examine the size and shape of

Table 1: Determination of crystallite size of the ZrO_2 NPs.

Peak Position (2θ) (degree)	FWHM (β) (radian)	Grain Size 'D' (nm)	(hkl)	Average crystallite Size (nm)
30.18	0.63	13.03	(101)	10.80
35.11	0.72	11.56	(110)	
50.28	1.02	8.60	(112)	
59.94	0.91	10.03	(211)	

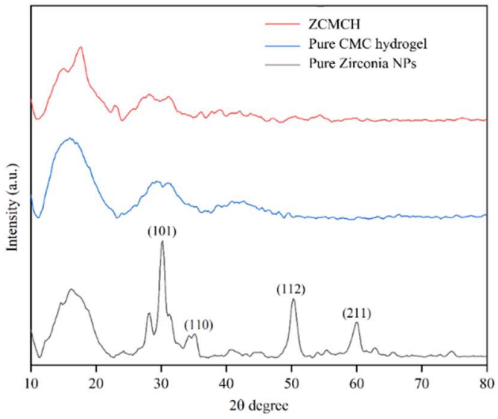

Figure 7: XRD patterns of ZCMCH, CMC hydrogel, and ZrO_2 NPs.

ZrO_2 NPs infused in CMC hydrogel[28]. The surface morphology of the ZrO_2 incorporated CMC hydrogel, together with the corresponding particle size distribution. The SEM micrograph (Figure 8a) shows a rough, interconnected surface typical of cross-linked CMC networks, consistent with the fibrillar morphologies commonly reported for CMC-based hydrogel. The ZrO_2 nanoparticles appeared as bright, relatively spherical structures embedded within the matrix, which aligned with the known SEM characteristics of ZrO_2 nanoparticles synthesized *via* sol-gel and related methods[29]. SEM image demonstrated that metal oxide nanoparticles can be homogeneously distributed within carboxymethyl cellulose matrices when strong polymer particle interactions occur, minimizing agglomeration and enhancing morphological stability[30]. For example, homogeneous dispersion of ZnO nanoparticles in CMC hydrogel was observed and attributed to the interaction between the nanoparticle surface and polymer chains, which prevents cluster formation and promotes stability within the matrix [30, 31].

In Figure 8a, no pronounced nanoparticle agglomeration was observed in the hydrogel sample, suggesting that the CMC hydrogel network effectively stabilized ZrO_2 nanoparticles during synthesis. Comparable behaviour was reported in other CMC nanocomposite systems, where the polymer matrix restricted nanoparticle mobility and enabled distribution in metal oxide polymer nanocomposites[27].

The histogram analysis revealed an average particle

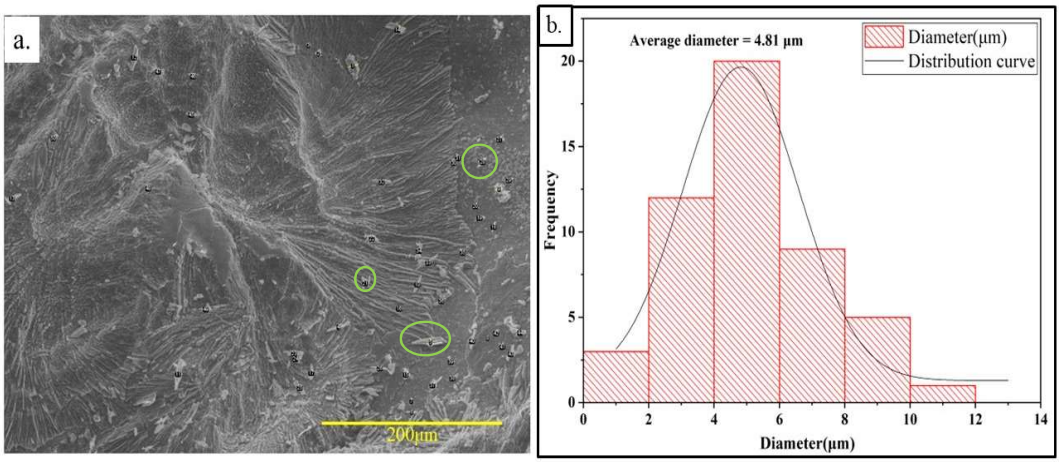

Figure 8: Morphological analysis (a) SEM image of ZrO_2 NPs infused in CMC hydrogel and (b) Histogram of size distribution of NPs on the hydrogel surface.

diameter of 4.81 µm, which is larger than the XRD-derived crystallite size of 10.80 nm. This difference is attributable to the fact that XRD measures the crystalline domains of nanoparticles in a dry powder state. In contrast, SEM captures agglomerated nanoparticle clusters within the hydrogel matrix[32, 33]. These interactions may be driven by high surface energy and van der Waals interactions between the hydrogel network and ZrO_2 nanocrystalite. The two values are complementary as the XRD result confirms the nanocrystalline nature of the synthesized ZrO_2, while the SEM histogram reflects the interactive behavior of nanocrystallites within the CMC polymer matrix[34, 35]. Such dispersion and distribution were relevant for enhanced interfacial contact, which is favourable for applications involving surface-dependent phenomena[30, 31].

Antimicrobial activity

Antibacterial Analysis

Using the Agar diffusion method, ZrO_2 NPs-infused CMC hydrogel exhibits activity against the bacterial pathogens *B. subtilis* and *E. coli*. Table 2 displays the zone of inhibition values found for CMC hydrogel infused with ZrO_2 NPs. The sample showed a substantial growth-inhibitory impact against both bacteria. The zone of inhibition of ZrO_2 nanoparticle-infused CMC hydrogel against *E. coli* bacteria was 1.6 cm, and the same result was observed against *B. subtilis* bacteria, as shown in Figure 9. According to the cited literature, a similar property has been demonstrated for ZrO_2 NPs[22, 28, 36, 37].

Antifungal Analysis

ZrO_2 NPs infused CMC hydrogel exhibited antifungal activity by effectively inhibiting the growth of *C. albicans* in the antifungal images depicted in Figure 10. Their increased surface area exhibited a substantial inhibitory effect against fungal strains. The zone of inhibition of ZrO_2 NPs infused CMC hydrogel against *C. albicans* bacteria was 1.4 cm, as mentioned in Figure 10. The antifungal activity of zirconia nanoparticles has been reported in the literature[28].

Table 2 illustrates the visual assessment of the inhibition zone for bacterial and fungal growth evaluated for the standard (Kanamycin) and ZCMCH.

Table 2: The zone of inhibition of organisms in ZCMCH.

Samples	*E. coli* (ATCC 8739)	*B. subtilis* (ATCC 6051)	*C. albicans* (ATCC 2091)
ZCMCH	1.6 cm	1.6 cm	1.4 cm
Positive control (c+)	2.6 cm	2.5 cm	2.5 cm

Conclusion

ZrO_2 NPs were successfully synthesized using the sol-gel method and modified with biocompatible citric and ascorbic acids to enhance their dispersion and compatibility within polymeric systems. The ZrO_2 NPs, functionalized with CA and AA for enhanced bifunctionality, were

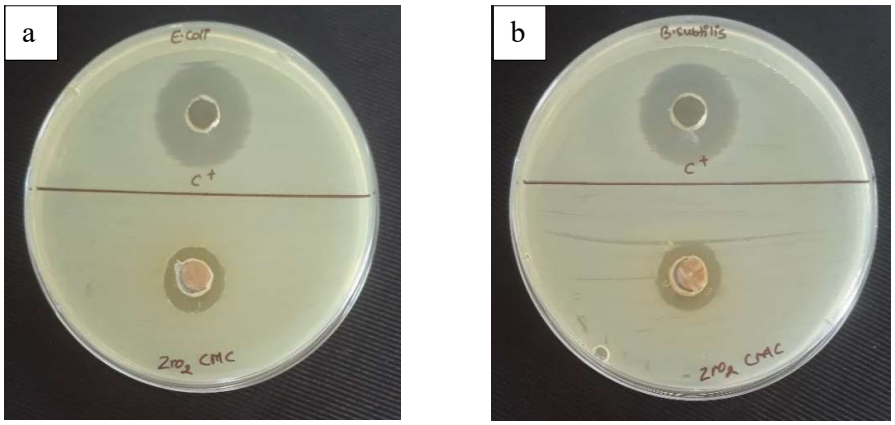

Figure 9: Antibacterial activity of ZrO_2 NPs infused CMC hydrogel a) E. coli b) B. subtilis.

Figure 10: Antifungal activity of ZrO_2 NPs infused CMC hydrogel against *Candida albicans*

incorporated into the CMC hydrogel matrix. The structural and morphological properties of the NPs and hydrogel were characterized using a range of analytical techniques, including UV-Visible Spectroscopy, FTIR, XRD, and SEM.

FTIR spectra displayed characteristic absorption peaks in the range of 480–750 cm^{-1}, confirming the presence of Zr-O vibrations. XRD analysis indicated a tetragonal crystal structure with an average crystallite size of 10.80 nm. SEM imaging revealed a homogeneous distribution of ZrO_2 NPs within the CMC hydrogel network. The combined results from FTIR, XRD, and SEM confirmed the successful synthesis and integration of ZrONPs within the CMC hydrogel. Furthermore, the antimicrobial performance of the ZrO_2-infused CMC hydrogel was evaluated and demonstrated significant antibacterial and antifungal activity. This suggests that the incorporation of ZrO_2 NPs enhances the functional properties of CMC hydrogel, making them potential material for antimicrobial applications.

Data Availability Statement

Data will be made available anytime on request.

Acknowledgements

The authors gratefully acknowledge Vyas Municipality, Tanahun, for funding support. The authors thank the Nepal Academy of Science and Technology (NAST) for XRD, Prof. Dr. Holger Schönherr, Department of Chemistry, University of Siegen, Germany, for SEM results, Research Centre for Applied Science and Technology (RECAST) for FTIR, and Himalaya Research Institute for Biotechnology for Antimicrobial tests.

Conflict of Interest

The authors declare no conflict of interest.

References

[1] Hebeish, A., Hashem, M., Abd El-Hady, M. M. and Sharaf, S. 2013. Development of CMC hydrogels loaded with silver nanoparticles for medical applications. *Carbohydrate polymers*. **92**(1): 407-413. Doi: https.//doi.org/10.1016/j.carbpol.2012.08.094.

[2] Kaczmarek, B., Nadolna, K. and Owczarek, A. 2020. The physical and chemical properties of hydrogels based on natural polymers. *Hydrogels based on natural polymers, Poland*.

[3] Ciolacu, D. E. and Suflet, D. M. 2018. Cellulose-based hydrogels for medical/pharmaceutical applications. In Biomass as renewable raw material to obtain bioproducts of high-tech value. *Elsevier. Romania*

[4] Biswal, D. R. and Singh, R. P. 2004. Characterisation of carboxymethyl cellulose and polyacrylamide graft copolymer. *Carbohydrate polymers*. **57**(4): 379-387. Doi: https.//doi.org/10.1016/j.carbpol.2004.04.020.

[5] Choe, D., Kim, Y. M., Nam, J. E.; Nam, K., Shin, C. S. and Roh, Y. H. 2018. Synthesis of high-strength microcrystalline cellulose hydrogel by viscosity adjustment. *Carbohydrate Polymer*. **180**: 231–237. Doi: https.//doi.org/10.1016/j.carbpol.2017.10.017.

[6] Reza, A. T. and Nicoll, S. B. 2010. Characterization of novel photocrosslinked carboxymethylcellulose hydrogels for encapsulation of nucleus pulposus cells. *Acta biomaterialia*. **6**(1): 179-186. Doi: https.//doi.org/10.1016/j.actbio.2009.06.004.

[7] Zainal, S. H., Mohd, N. H., Suhaili, N., Anuar, F. H., Lazim, A. M. and Othaman, R. 2021. Preparation of cellulose-based hydrogel: A review. *Journal of Materials Research and Technology*. **10**: 935-952. Doi: https.//doi.org/10.1016/j.jmrt.2020.12.012.

[8] Kanikireddy, V., Varaprasad, K., Jayaramudu, T., Karthikeyan, C., and Sadiku, R. 2020. Carboxymethyl cellulose-based materials for infection control and wound healing: A review. *International Journal of Biological Macromolecules*. **164**: 963-975. Doi: https.//doi.org/10.1016/j.ijbiomac .2020.07.160.

[9] Zheng, W.J., Gao, J., Wei, Z., Zhou, J. and Chen, Y. M. 2015. Facile fabrication of self-healing carboxymethyl cellulose hydrogels. *European Polymer Journal*. **72**: 514-522. Doi: https.//doi.org/10.1016/j.eurpolymj.2015.06.013.

[10] Kono, H. 2014. Characterization and properties of carboxymethyl cellulose hydrogels crosslinked by polyethylene glycol. *Carbohydrate polymers*. **106**: 84-93. Doi: https://doi.org/10. 1016/j.carbpol.2014.02.020

[11] Sigwadi, R., Dhlamini, M., Mokrani, T. and Nemavhola, F. 2019. Preparation of a high surface area zirconium oxide for fuel cell application. *International Journal of Mechanical and Materials Engineering*. **14**(1): 5. Doi: https.//doi.org/10.1186/s40712-019-0102-9.

[12] Mallakpour, S. and Nezamzadeh Ezhieh, A. 2018. Citric acid and vitamin C as coupling agents for the surface coating of ZrO_2 nanoparticles and their behavior on the optical, mechanical, and thermal properties of poly(vinyl alcohol) nanocomposite films. *Journal of Polymers and the Environment.* **26**(7): 2813-2824. Doi: https.//doi.org/10.1007/s10924-017-1170-7.

[13] Kango, S., Kalia, S., Celli, A., Njuguna, J., Habibi, Y. and Kumar, R. 2013. Surface modification of inorganic nanoparticles for development of organic–inorganic nanocomposites—A review. *Progress in polymer science.* **38**(8): 1232-1261. Doi: https.//doi.org/10.1016/j.progpolymsci.2013.02.003.

[14] Rai, N., Shah, S., Joshi, R. and Pandit, R. 2021. Green synthesis and characterization of Zirconia nanoparticles using extract of citrus sinensis peels and its comparative antibacterial activity with Cefotaxime. *Spectrum of Emerging Sciences*. **1**(1): 36-41.

[15] Li, S., Dong, S., Xu, W., Tu, S., Yan, L., Zhao, C., Ding, J. and Chen, X. 2018. Antibacterial Hydrogels. *Advanced science*. **5**(5): 1700527. Doi: https.//doi.org/10.1002/advs.201700527.

[16] Yang, K., Han, Q., Chen, B., Zheng, Y., Zhang, K., Li, Q. and Wang, J. 2018. Antimicrobial hydrogels: promising materials for medical application. *International journal of nanomedicine*. **13**: 2217-2263. Doi: https://doi.org/10.2147/IJN.S154748

[17] Tabassum, N., Kumar, D., Verma, D., Bohara, R. A. and Singh, M. P. 2021. Zirconium oxide (ZrO_2) nanoparticles from antibacterial activity to cytotoxicity: A next-generation of multifunctional nanoparticles. *Materials Today Communications.* **26**: 102156. Doi: https.//doi.org/10.1016/j.mtcomm.2021.102156.

[18] Dwivedi, R., Maurya, A., Verma, A., Prasad, R. and Bartwal, K.S. 2011. Microwave assisted sol–gel synthesis of tetragonal zirconia nanoparticles. *Journal of Alloys and Compounds*. **509**(24): 6848-6851. Doi: https.//doi.org/10.1016/j.jallco m.2011.03.138.

[19] Mallakpour, S. and Nezamzadeh Ezhieh, A. 2018. Surface modification of ZrO_2 nanoparticles with biosafe coupling agents, preparation of poly (vinyl pyrrolidone) nanocomposites: optical, thermal, and morphological studies. *Advances in Polymer Technology*. **37**(2): 586-595. Doi: https.//doi.org/10.1002/adv.21699.

[20] Raafat, A. I., Eid, M. and El-Arnaouty, M. B. 2012. Radiation synthesis of superabsorbent CMC based hydrogels for agriculture applications. *Nuclear Instruments and Methods in Physics Research B.* **283**: 71-76. Doi: https.//doi.org/10.1016/j.nimb.2012.04.011.

[21] Georgieva, I., Danchova, N., Gutzov, S. and Trendafilova, N. 2012. DFT modeling, UV-Vis and IR spectroscopic study of acetylacetone-modified zirconia sol-gel materials. *Journal of molecular modeling.* **18**(6): 2409-2422. Doi: https://doi.org/10.1007/s00894-011-1257-3.

[22] Kumaresan, M., Anand, K.V., Govindaraju, K., Tamilselvan, S. and Kumar, V. G. 2018. Seaweed Sargassum wightii mediated preparation of zirconia (ZrO_2) nanoparticles and their antibacterial activity against gram positive and gram negative bacteria. *Microbial pathogenesis*. **124**: 311-315. Doi: https.//doi.org/10.1016/j.micpath.2018.08.060.

[23] Mallakpour, S. and Nezamzadeh Ezhieh, A. 2017. A simple and environmentally friendly method for surface modification of ZrO_2 nanoparticles by biosafe citric acid as well as ascorbic acid (vitamin C), and its application for the preparation of poly (vinyl chloride) nanocomposite films. *Polymer Composites*. **38**(8): 1756-1765. Doi: https://doi.org/10.1002/pc.23746.

[24] Zare-Akbari, Z., Farhadnejad, H., Furughi-Nia, B., Abedin, S., Yadollahi, M. and Khorsand-Ghayeni, M. 2016. PH-sensitive bionanocomposite hydrogel beads based on carboxymethyl cellulose/ZnO nanoparticle as drug carrier. *International journal of biological macromolecules*. **93**: 1317-1327. Doi: https.//doi.org/10.1016/j.ijbiomac.2016.09.110.

[25] Gholamali, I. and Yadollahi, M. 2020. Doxorubicin-loaded carboxymethyl cellulose/Starch/ZnO nanocomposite hydrogel beads as an anticancer drug carrier agent. *International Journal of Biological Macromolecules*. **160**: 724-735. Doi: https.//doi.org/10.1016/j.ijbiomac.2020.05.232.

[26] Cyriac, B. 2023. Zirconia: Synthesis and Characterization. In: AI-Naib, U.M.B. (Ed.), *Zirconia – New Advances, Structure, Fabrication and Applications*. IntechOpen, London. Doi: https://doi.org/10.5772/intechopen.111737.

[27] Rasoulzadeh, M. and Namazi, H. 2017. Carboxymethyl cellulose/graphene oxide bio-nanocomposite hydrogel beads as anticancer drug carrier agent. *Carbohydrate Polymers*. **168**: 320-326. Doi: https.//doi.org/10.1016/j.carbpol.2017.03.014.

[28] Gowri, S., Gandhi, R. R. and Sundrarajan, M. 2014. Structural, optical, antibacterial, and antifungal properties of zirconia nanoparticles by biobased protocol. *Journal of Materials Science & Technology*. **30**(8): 782-790. Doi: https.//doi.org/10.1016/j.jmst.2014.03.002.

[29] Jiang, H., Zhang, G., Feng, X., Liu, H., Li, F., Wang, M. and Li, H. 2017. Room-temperature self-healing tough nanocomposite hydrogel crosslinked by zirconium hydroxide nanoparticles. *Composites Science and Technology*. **140**: 54-62. Doi: https.//doi.org/10.1016/j.compscitech.2016.12.027.

[30] Yadollahi, M., Gholamali, I., Namazi, H. and Aghazadeh, M. 2015. Synthesis and characterization of antibacterial carboxymethyl cellulose/ZnO nanocomposite hydrogels. *International journal of biological macromolecules*. **74**: 136-141. Doi: https://doi.org/10.1016/j.ijbiomac.2014.11.032.

[31] Zafar, A., Khosa, M. K., Noor, A., Qayyum, S. and Saif, M. J. 2022. Carboxymethyl cellulose/gelatin hydrogel films loaded with zinc oxide nanoparticles for sustainable food packaging applications. *Polymers*. **14**(23): 5201. Doi: https:// doi.org/10.3390/polym14235201.

[32] Graebin, A. P., Bonnaud, L., Persenaire, O., Murariu, O., Dubois, P., Rocha, Z. N. D. and Basso, N. R. D. S. 2015. Polyethylene-polyaniline nanofiber composites: evaluation of experimental conditions of in situ polymerization. *Materials Research*. **18**(suppl 2): 121-126. Doi: https://doi.org/10.1590/1516-1439.348914.

[33] Jensen, H., Pedersen, J. H., Jorgensen, J. E., Pedersen, J. S., Joensen, K. D., Iversen, S. B. and Sogaard, E. G. 2006. Determination of size distributions in nanosized powders by TEM, XRD, and SAXS. *Journal of Experimental Nanoscience*. **1**(3): 355–373. Doi: https://doi.org/10.1080/17458080600752482.

[34] Hiremath, A., Murthy, A. A., Thipperudrappa, S. & KN, B. 2021. Nanoparticles filled polymer nanocomposites: a technological review. *Cogent engineering*. **8**(1): 1991229. Doi: https://doi.org/10.1080/23311916.2021.1991229.

[35] Arul Vasanthi, T. and Balakrishnan, G. 2020. Synthesize of zirconium oxide (ZrO_2) nanoparticles and characterization. *Malaya Journal of Matematik*. **S**(2): 4955–4959. Doi: https://doi.org/10.26637/MJM0S20/1278.

[36] Hamid, L. L., Zakir, R. S., Abdel Rahman, N. M., Idrahim, R. H. and Abdel Rahman, S. M. 2025. construction and characterization of polyethylene glycol/sodium alginate hydrogel loaded with zirconia nanoparticles: potential antibacterial and antibiofilm agent to inhibit dental caries in vitro and in vivo. *Microsc Res Tech*. **88**: 2268-2284. Doi: https://doi.org/10.1002/jemt.24860.

[37] Pushpalatha, S., Arularasu, M. V., Palanivel, C., Rajendran, T. V. and Manikandan, A. 2025. Green synthesis of cellulose/ZrO_2 nanocomposite: assessment of antibacterial and photocatalytic activity. *Biomass Conversion and Biorefinery*, **15**(19): 26687-26694. Doi: https://doi.org/10.1007/s13399-024-05708-w.